*Progress In Electromagnetics Research C, Vol. 107, 157–171, 2021*

# Mutual Coupling Reduction in Patch Antenna Array Using Combination of Shorting Pins and Metallic Walls

**Irfan A. Tunio*, Yann Mahé, Tchanguiz Razban, and Bruno Froppier**

**Abstract**—A method of loaded patch antennas with shorting pins and erected walls in between patch antenna arrays is introduced to reduce surface wave and free space wave coupling in both $E$ and $H$-planes. This simple technique works equally well in both orientations by reducing coupling up to $-19\,\mathrm{dB}$ and $-15\,\mathrm{dB}$ (measured value) in $E$-plane and $H$-plane, respectively, as compared to a conventional patch antenna array. The scattering parameters are studied, and conclusions are made on amounts of mutually coupled power and the bandwidth of the rejection band ($S_{12}$). A parametric study of the variation in the level of mutual coupling with respect to height of the wall has been carried out in both $E$ and $H$-planes. The simulation results are well verified through measurements.

## 1. INTRODUCTION

Ubiquitous use of patch antennas in wireless industry shows their promising merits such as low profile, light weight, low cost, easy manufacture, being conformal, and easy integration to microwave circuits. Contrary to merits, patch antennas suffer from some drawbacks such as excitation of surface waves, low efficiency, and low gain. To overcome these issues, various techniques such as thick-low permittivity substrate, stacked configurations, ferrite composition, combination of slot-slits, and resonant cavity antenna can be considered [1–5]. On the other hand, multiple antennas working together, called arrays, can be utilized for high gain, beam steering, multiple-input multiple-output (MIMO), diversity purposes, etc. When patch antennas are aimed for arrays on a thick and lossy substrate, the design becomes more critical. In such a case, the issue of mutual coupling starts to dominate in two different ways as follows [6, 7]:

- Coupling through surface waves,
- Coupling through free space waves.

Either of these coupling mechanisms may dominate over the other depending upon antenna type, substrate width, ground plane, and modes excited by the patch. However, in printed antennas, surface waves may dominate if the substrate thickness is in accordance with condition (1) [8].

$$\text{Substrate thickness} \geq \frac{0.3\lambda_0}{\left(2\pi\sqrt{\epsilon_r}\right)} \tag{1}$$

Here, $\lambda_0$ is the wavelength in free space, and $\epsilon_r$ is the relative permittivity of substrate.

The presence of this unwanted coupling in an array changes the terminal impedances of the antennas, reflection coefficients, array gain, beamwidth, etc. To overcome the problem of mutual coupling, various techniques have been proposed to eliminate or reduce the effect of coupling in antenna arrays. Most of these techniques are designed to reduce coupling either in $E$-plane [9–16] or in $H$-plane

*Received 28 August 2020, Accepted 26 November 2020, Scheduled 7 December 2020*
* Corresponding author: Irfan Ali Tunio (irfan-ali.tunio@etu.univ-nantes.fr).
The authors are with the IETR, University of Nantes, Nantes 44306, France.

orientation [17–19]. The techniques that work well in $E$-plane orientation do not work in $H$-plane. The same is true for reduction techniques in $H$-plane orientation. To add more, there are some examples where the authors have shown to reduce coupling in both $E$- and $H$-plane orientations [20–22]. However, they have used altogether different methods to do so because of the nature of the coupling. In addition to that, unfortunately, some of these approaches demonstrate narrow bandwidth of rejection band ($S_{12}$) which do not cover the operational bandwidth of the antennas. Table 1 provides a summarised comparative analysis among some of the decoupling methods cited above.

In this paper, we propose a technique to reduce coupling by using the combination of metallic pins and metallic wall barriers. Metallic pins are shorted in between the patch and the ground in order to suppress surface waves and radiations in horizontal directions. Later, in arrays, metallic barriers are inserted to further reduce the effect of free space wave coupling. This technique works equally well in both $E$- and $H$-plane orientations, and the array can be extended to larger planar geometry. Apart from coupling suppression better than $-40$ dB (required in most applications) at the resonant frequency, this technique has an advantage of wide-band rejection characteristics of transmission coefficient.

In Section 2, single conventional and pin loaded patch antenna is designed which is later used in Section 3 to build antenna arrays in $E$-plane and $H$-plane orientations with decoupling mechanism. Section 4 concludes the discussion.

## 2. SINGLE PATCH ANTENNA DESIGN OPTIMISATION

### 2.1. Conventional Patch Antenna and Pin Loaded Patch Antenna Design

We design and optimize a single patch antenna at operating frequency of 5.69 GHz. Once it is optimized, the antenna is then put in array combinations. Here, this frequency is arbitrarily chosen and can be used for WLAN applications, but the technique that we later introduce can be extended to any application.

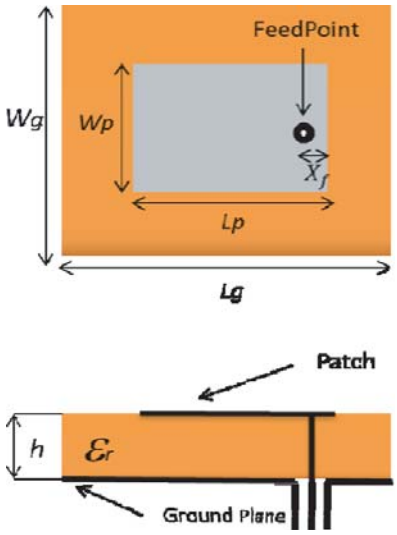


**Figure 1.** Conventional patch antenna with top and side view with optimized parameters in $mm$: Length of the patch ($Lp$) = 11.4, width of the patch ($Wp$) = 9.5, co-axial feed point distance from the edge of the patch ($X_f$) = 3.9, height of the substrate ($h$) = 1.6, substrate material is FR4 epoxy with $\epsilon_r = 4.4$ and $\tan\delta = 0.02$, patch and ground material is copper (35 µm Thick), substrate and ground length ($Lg$) = 65.4, substrate and ground width ($Wg$) = 63.5.

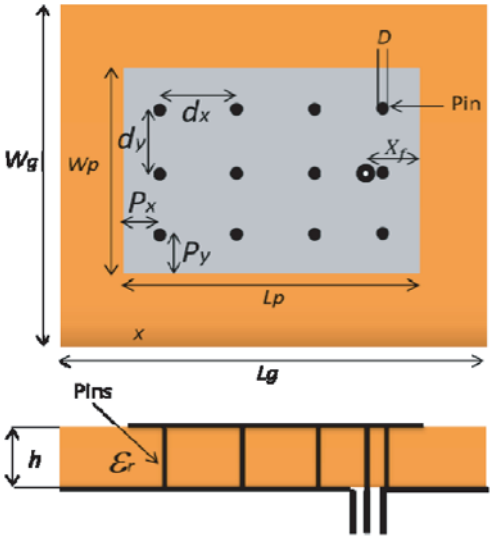


**Figure 2.** Pin loaded patch antenna with top side view with optimized parameters in mm: Length of the patch ($Lp$) = 31, width of the patch ($Wp$) = 25, co-axial feed point distance from the edge of the patch ($X_f$) = 4.3, height of the substrate ($h$) = 1.6, diameter of the pin ($D$) = 1, Inter distance between the pins ($dx$ and $dy$) = 9, the distance of pins from the patch edge to pins along $X$-axis ($P_x$) = 2.5 and along $Y$-axis ($P_y$) = 3.5, total number of pins = $12(3 \times 4)$.

**Table 1.** Comparison between different mutual coupling reduction techniques.

| Paper | Technique | $E/H$ plane | MC ($S_{12}$) in dB | Centerto Center distance | Antenna size in $\lambda_0$: Length ($L$), Width ($W$), Height ($h$) | BW of rejection band ($S_{12}$) | Design complexity |
|---|---|---|---|---|---|---|---|
| [9] | DGS | $E$ | $-27$ | $0.75\lambda_0$ | $L = 0.137$, $W = 0.134$, $h = 0.035$ | Narrow | Moderate |
| [10] | DGS | $E$ | $-33$ | $0.5\lambda_0$ | $L = 0.132$, $W = 0.134$, $h = 0.04$ | Narrow | Low |
| [11] | EBG | $E$ | $-25$ | $0.75\lambda_0$ | $L = 0.135$, $W = 0.077$, $h = 0.038$ | Wide | Low |
| [12] | EBG | $E$ | $-40$ | $0.75\lambda_0$ | $L = 0.35$, $W = 0.35$, $h = 0.085$ | Wide | Low |
| [16] | EBG + Cuts | $E$ | $-48$ | $1\lambda_0$ | $L = 0.7$, $W = 0.625$, $h = 0.0298$ | Wide | Low |
| [17] | U-section | $H$ | $-39$ | $0.6\lambda_0$ | $L = 0.38$, $W = 0.316$, $h = 0.065$ | Narrow | Moderate |
| [18] | Wall | $H$ | $-40$ | $0.25\lambda_0$ | $L = 0.235$, $W = 0.191$, $h = 0.005$ | Wide | Low |
| [19] | Wall | $H$ | $-54$ | $0.28\lambda_0$ | $L = 0.261$, $W = 0.251$, $h = 0.029$ | Wide | Low |
| [21] | Rectangular slot | $E$-$H$ | $-37$ | $0.5\lambda_0$ | $L = 0.31$, $W = 0.31$, $h = 0.053$ | Narrow | Moderate |
| [22] | Metasurface Superstrate | $E$-$H$ | $-25$ | $0.43\lambda_0$ | $L = 0.239$, $W = 0.237$, $h = 0.029$ | Narrow | High |
| This paper | Pins + wall | $E$-$H$ | $-40$ | $0.7\lambda_0$ | $L = 0.574$, $W = 0.462$, $h = 0.0296$ | Wide | Low |

Single conventional patch antenna along with its optimized parameters is presented in Figure 1.

The antenna has been simulated in HFSS Ansys with optimized return loss of $-28.44$ dB as shown in Figure 3 (Dashed red curve). Figure 4 shows the radiation pattern of the conventional patch antenna where 4.96 dBi of directivity is observed in the broadside direction ($\theta = 0^\circ$).

We design another single patch antenna loaded with shorting pins to resonate at the same frequency as previously. The idea behind this technique is to modify the characteristics of the substrate so that

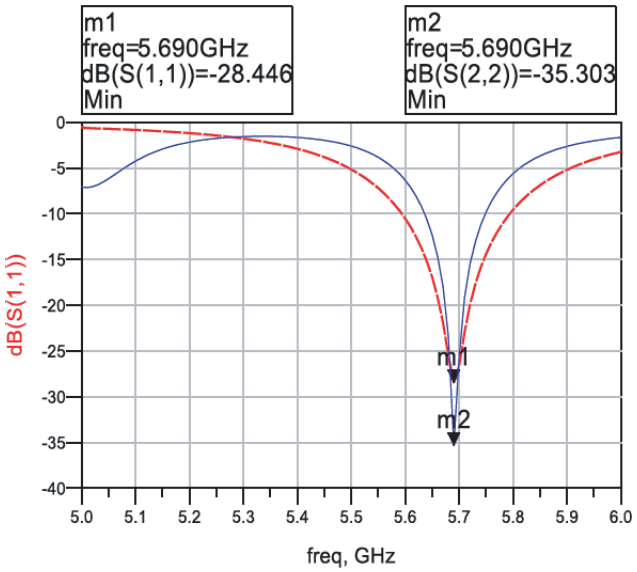


**Figure 3.** Simulated return loss of conventional patch antenna (dashed red curve) and pin loaded patch antenna (solid blue curve).

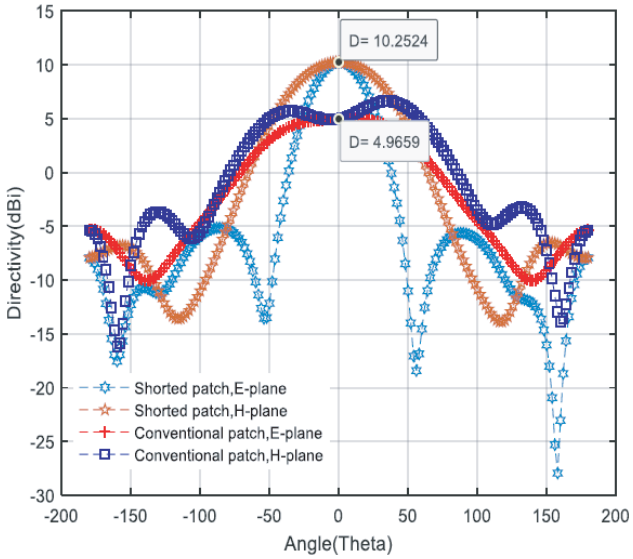


**Figure 4.** 2D Radiation pattern of conventional and pin loaded patch antenna showing directivity in $E$- and $H$-plane orientations.

it does not excite sufficient surface waves such that the patch can later be used in array combinations.

Shorting pins in a microstrip patch antenna can be preferred to chip inductors and capacitors due to their lower losses and ease of implementation. Therefore, the use of shorting pins in patch antennas has revealed a variety of applications. For instance, shorting pins can be used to enhance gain [23], reduce cross polarization [24], reduce resonant frequency in order to make antenna more compact [25], make antenna dual bands [26–28], increase impedance bandwidth [29], cancel out polarization currents in substrates [8], suppress specific modes for isolation enhancement [30], and cancel out harmonic radiations [31].

Indeed in patch antennas, polarization currents are initiated due to the presence of surface waves which are guided by the dielectric substrate to the air interface. Due to these polarization currents, a strong resonant electrical field exists inside the dielectric under the patch. At the edge of the patch, this electrical field is strong, and a part radiates. Due to the dielectric to air interface, a part of the bent fields propagate and couple to the adjacent antennas: this is the main contributor of the so-called surface waves.

In order to cancel out the effect of polarization current, a counter phased mechanism is required. In our design, this has been achieved through the shorting pins placed at proper locations in between the patch and the ground. This mechanism introduces extra inductive polarization currents which compensate existing capacitive polarization currents in the dielectric [8]. In this way, strong surface waves can be suppressed.

Figure 2 shows the proposed patch antenna with compensated shorting pins. The position and dimensions of the pins are obtained from literature and optimization. The length and width of the patch are enlarged in order to compensate the effect of shorting pins. In order to have same frequency as that of conventional patch antenna, the new dimensions of the patch become almost $\sqrt{\varepsilon_r}$ times bigger than the conventional antenna printed on FR-4. Here, effective permittivity tends to be closer to relative permittivity making dielectric behave more like air cavity. In this way, the pin loaded patch antenna acts as though there is air dielectric as a new dielectric medium and hence considerably reducing surface waves. The optimized parameters of the pin loaded patch antenna are shown in the caption of Figure 2.

The pin loaded patch antenna has been simulated. Figure 3 shows the optimized return loss of the antenna (solid blue curve). Here, the pin loaded patch antenna presents a return loss of $-35.3$ dB at the same resonant frequency as that of conventional patch antenna. It can be observed through Figure 4 that the pin loaded patch antenna presents a directivity of 10.25 dBi which is almost 5.3 dB bigger than

a conventional patch antenna. Here, the cost of increased directivity in pin loaded patch antenna is its lower impedance bandwidth (almost 30% less than conventional patch antenna) (Figure 3).

In order to validate simulation results, conventional and pin loaded antennas have been manufactured as shown in Figures 5(a)–(b). The $S$-parameters of both antennas have been measured as shown in Figure 6. It can be observed that the manufactured antennas resonate slightly at different frequencies because of the inherent manufacturing tolerance. The conventional patch antenna resonates around 5.73 GHz with the return loss of −21.5 dB, and the pin loaded patch antenna resonates at 5.8 GHz with the return loss of −23.32 dB. This small variation of the resonant frequency will not affect the observance of our results in terms of reduction of mutual coupling in antenna arrays. Therefore, we would build arrays (both in $E$- and $H$-planes) with conventional and pin loaded patch antennas so that a comparison can be given.

Figures 7(a) and (b) show the measured radiation patterns of conventional and pin loaded patch antennas, respectively, in terms of gain magnitude (dBi) versus angles (Theta). Here, it can be observed that the antennas radiate optimally in co-polarization and minimum in cross-polarization at the broadside direction ($\theta = 0°$).

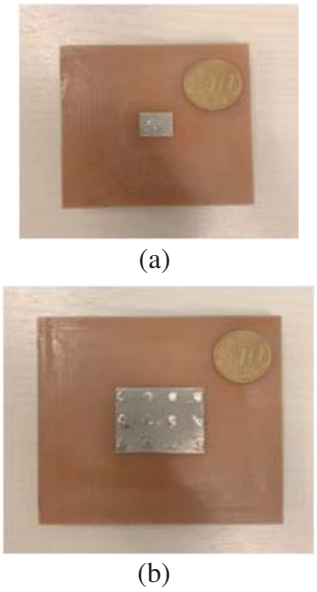


**Figure 5.** Laboratory prototypes of single: (a) Conventional patch antenna; (b) Pin loaded patch antenna.

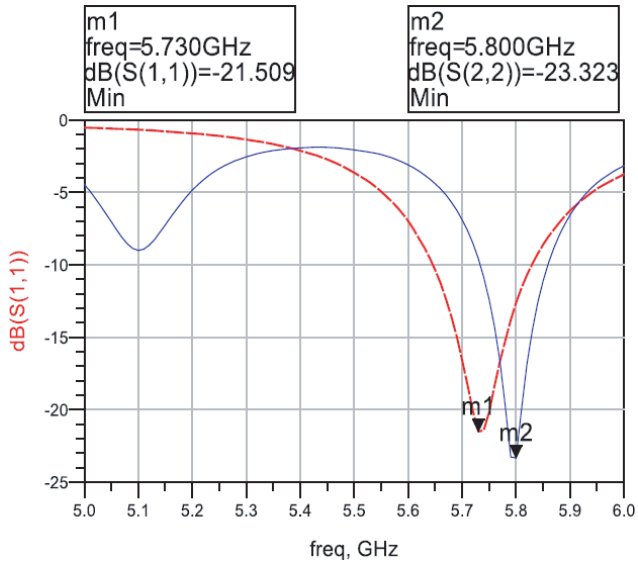


**Figure 6.** Measured return loss of conventional patch antenna (dashed red curve) and pin loaded patch antenna (solid curve).

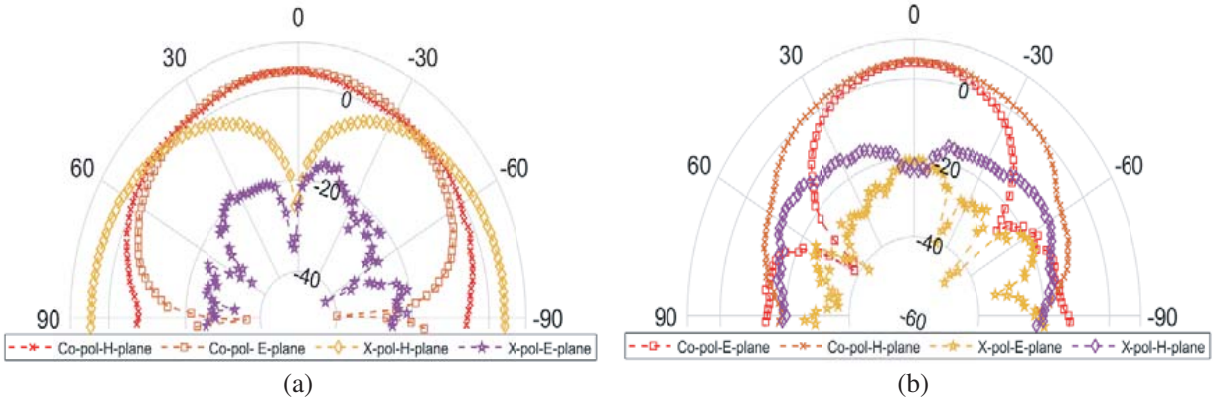


**Figure 7.** Measured radiation pattern of: (a) Conventional patch antenna; (b) Pin loaded patch antenna.

## 3. PATCH ANTENNA ARRAY ANALYSIS

After optimizing a single conventional patch antenna, an array with it can be constructed in both $E$- and $H$-planes so that, later on, we can compare them with those of pin loaded patch antennas.

### 3.1. 3D Simulation of Conventional Patch Antenna Array Oriented along $E$- and $H$-Planes

Two antenna elements arranged along $E$- and $H$-planes have been simulated as shown in Figure 8. The feed point distance is set at $0.7\lambda_0$ as a trade-off between mutual coupling and grating lobes in this particular design. The ground plane is extended $\lambda_0/2$ away in all directions from the antenna elements.

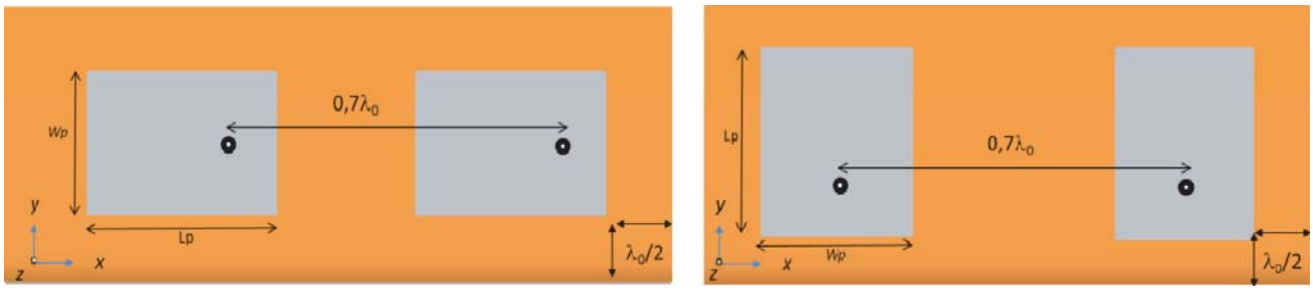


(a) (b)

**Figure 8.** Two element conventional patch antenna array oriented along: (a) $E$-plane; (b) $H$-plane.

The array is simulated, and its corresponding $S$-parameters are shown in Figure 9. The conventional antennas oriented along $E$- and $H$-planes present mutual couplings ($S_{12-21}$) approximately $-21.03$ dB and $-27.03$ dB, respectively. An impedance bandwidth ($|S_{11}$ & $S_{22}| < 10$ dB) approximately $\sim 180$ MHz and $\sim 200$ MHz is observed in $E$-plane and $H$-plane, respectively.

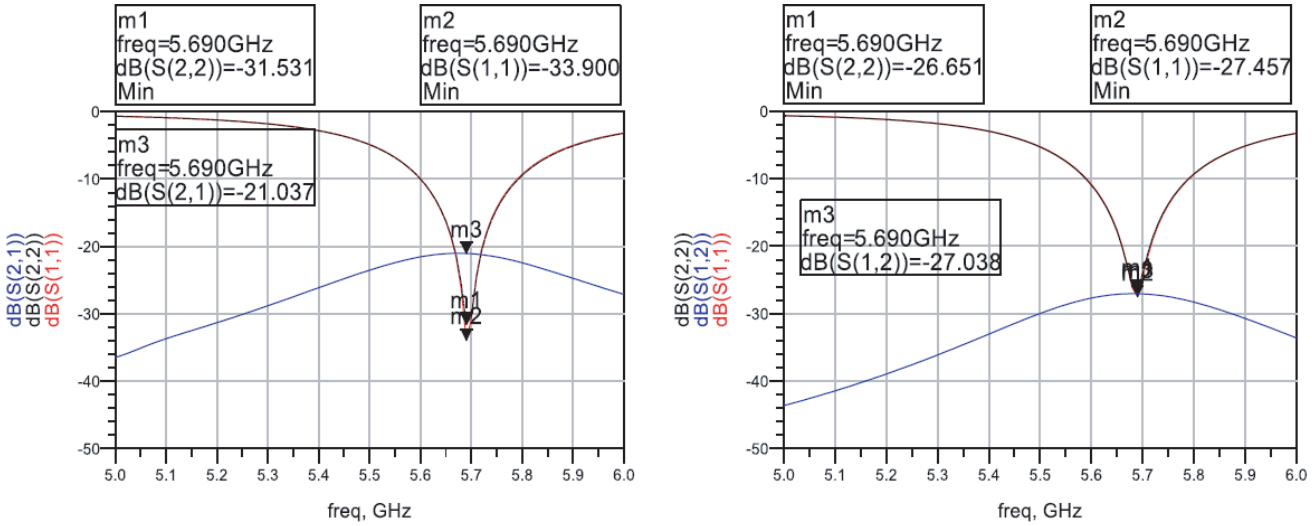


(a) (b)

**Figure 9.** Simulated $S$-parameters of two conventional patch antenna elements oriented along: (a) $E$-plane; (b) $H$-plane.

### 3.2. Realization of Conventional Patch Antenna Array Oriented along *E*- and *H*-Planes

The conventional patch antenna array arranged along $E$-plane and $H$-plane has been manufactured to validate 3D simulation results. Figure 10 shows the manufactured antenna array in both orientations. The conventional antennas oriented along $E$- and $H$-planes show mutual couplings ($S_{12-21}$) approximately $-21.56$ dB and $-29.50$ dB (Figure 11), respectively, which is almost the same as that obtained through simulations. It can be observed that the antennas in $E$-plane resonate slightly at higher frequency (5.71 GHz) than the reference antenna which is due to the manufacturing tolerance. Also in $H$-plane, one of the antennas resonates slightly lower (5.68 GHz) than the reference antenna which is again due to manufacturing tolerance. It can be seen that simulated and realized results show similarities between $E$- and $H$-plane configurations in terms of transmission coefficients and return losses.

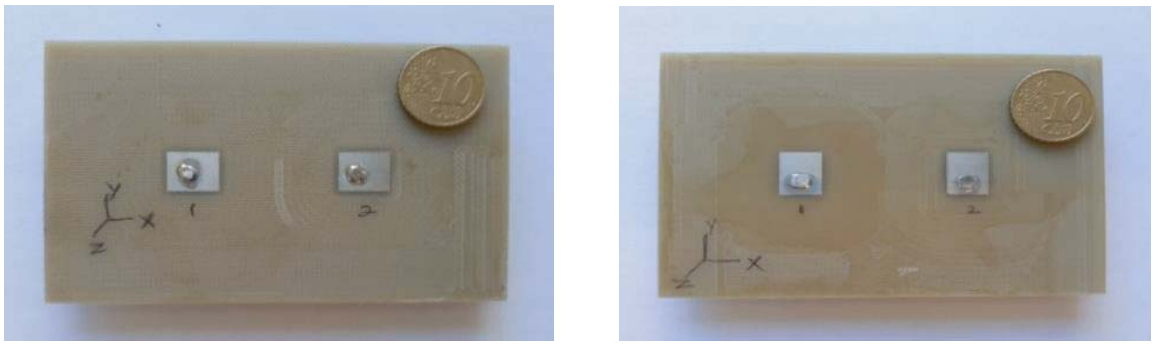

(a) (b)

**Figure 10.** Fabricated two element conventional patch antenna array oriented along: (a) $E$-plane; (b) $H$-plan.

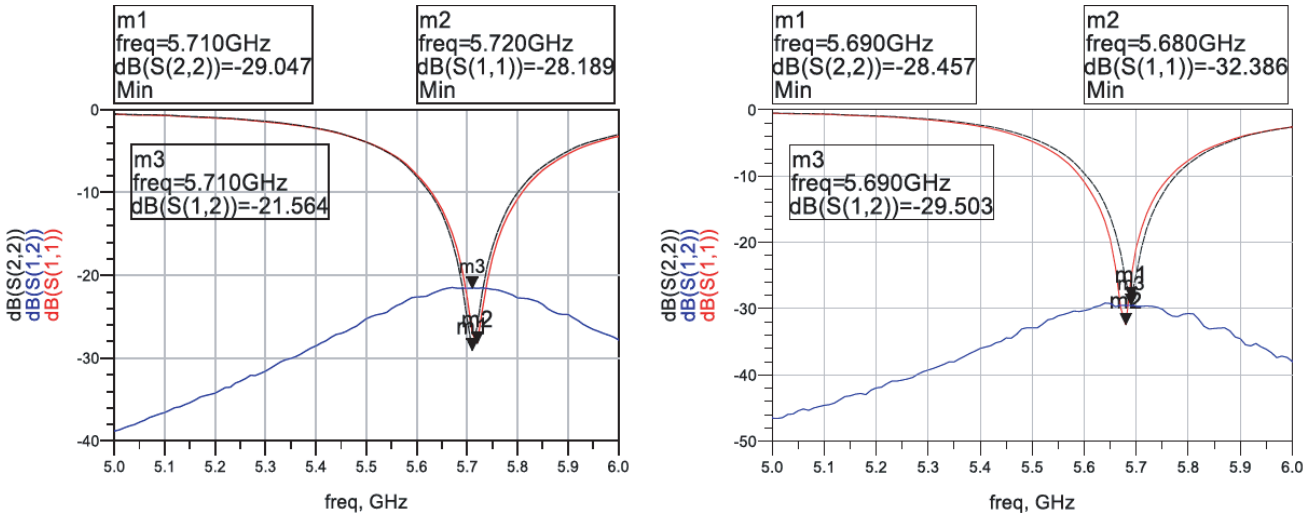


(a) (b)

**Figure 11.** Measured $S$-parameters of two conventional patch antenna array oriented along: (a) $E$-plane; (b) $H$-plane.

Figure 12 shows the measured radiation patterns of both configurations. In the case of a two antenna element array, the radiation pattern measurements are carried out in an anechoic chamber with the aid of power splitter to feed both antennas at the same time. It can be observed that the array radiates optimally in the co-polarization and remains under 20 dB in the cross-polarization (Broadside direction) in both planes of orientations.

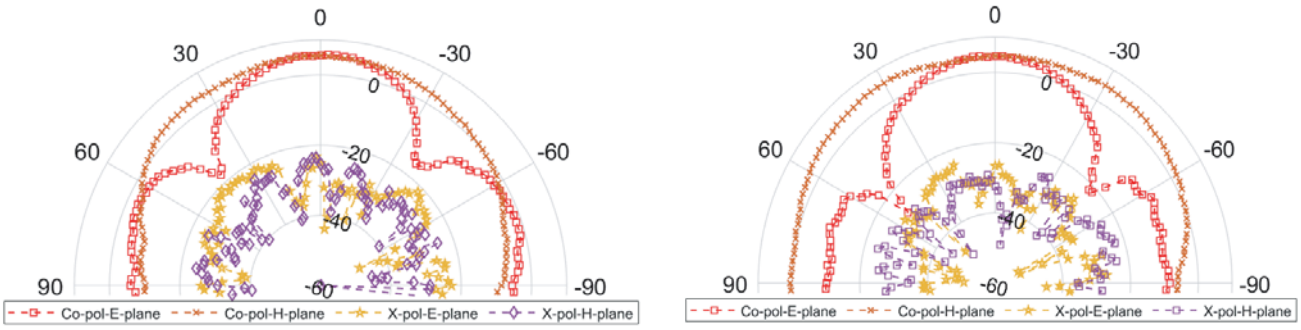


(a) (b)

**Figure 12.** Measured radiation pattern of two conventional patch antenna array oriented along: (a) $E$-plane; (b) $H$-plane.

### 3.3. 3D Simulation of Pin Loaded Patch Antenna Array Oriented along *E*- and *H*-Planes

Two element pin loaded patch antennas have been arranged according to $E$-plane and $H$-plane configurations as shown in Figure 13(a) and Figure 13(b), respectively. Both $E$-plane and $H$-plane

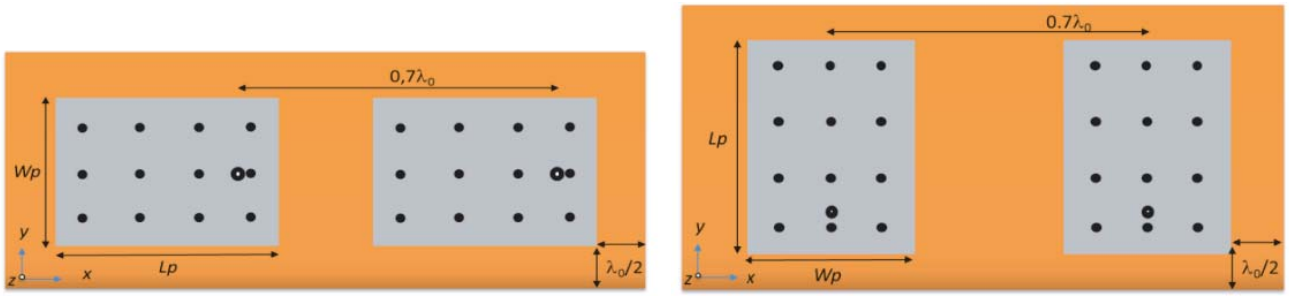


(a) (b)

**Figure 13.** Pin loaded two element antenna array oriented along: (a) $E$-plane; (b) $H$-plane.

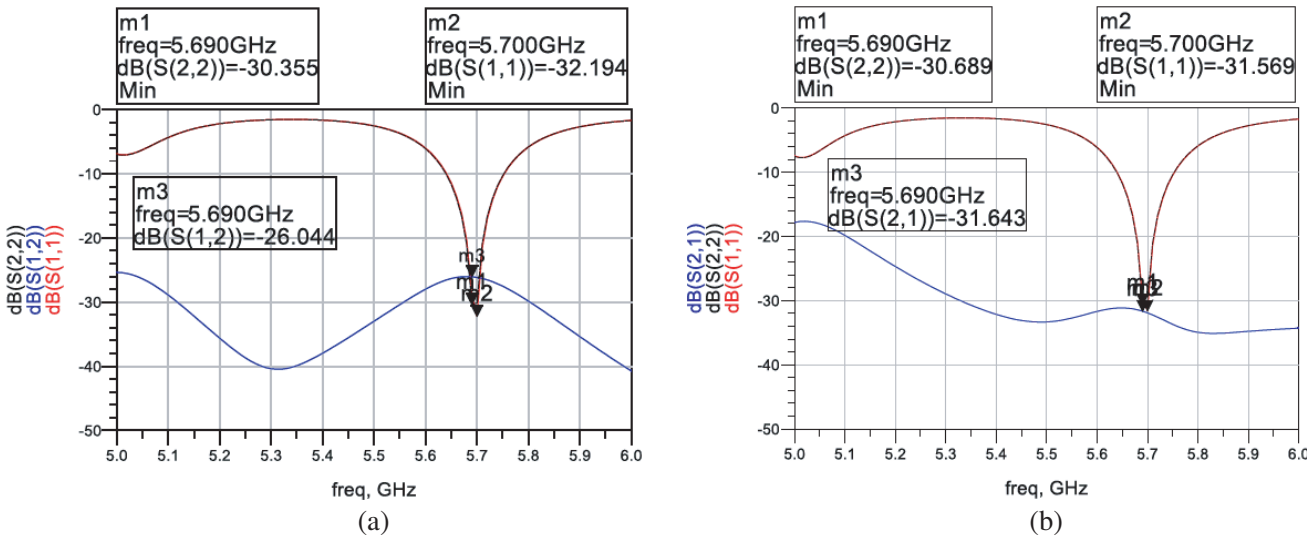


(a) (b)

**Figure 14.** Simulated $S$-parameters of pin loaded two element antennas oriented along: (a) $E$-plane; (b) $H$-plane.

configurations have been simulated, and their corresponding $S$-parameters are presented in Figure 14(a) and Figure 14(b), respectively. The pin loaded antennas oriented along $E$- and $H$-planes show mutual couplings ($S_{12–21}$) approximately $-26.04$ dB and $-31.64$ dB, respectively. It can be seen that antennas #1 and 2 resonate slightly at different frequencies in $E$- and $H$-planes. Despite having same parameters of both antennas, a slight variation in their resonant frequencies may have resulted due to the introduced mesh on each antenna.

At the resonant frequency, it can be observed that patch antennas loaded with pins present almost 5 dB and 4 dB less coupling than the conventional antenna array in $E$-plane and $H$-plane, respectively.

In order to reduce coupling further, we introduce metallic wall barriers in between antenna elements to suppress free space wave coupling among such pin loaded antenna elements.

### 3.4. 3D Simulation of Pin Loaded Patch Antenna Array with Metallic Wall Oriented along *E*- and *H*-Planes

In order to suppress free space wave coupling, a wall is erected in between the adjacent $E$- and $H$-plane coupled elements in the array. The wall structure proposed in this work is based on a copper sheet with the thickness ($W_w$) of 1 mm and height ($W_h$) of 25 mm (Figure 15). The wall structure is centered between two antenna elements and optimized in height and relative distance. The wall centered at the distance ($d$) of 3 mm (Figure 15(a)) and 7 mm (Figure 15(b)) along $E$- and $H$-planes, respectively, has been chosen to reduce coupling on a desired frequency band.

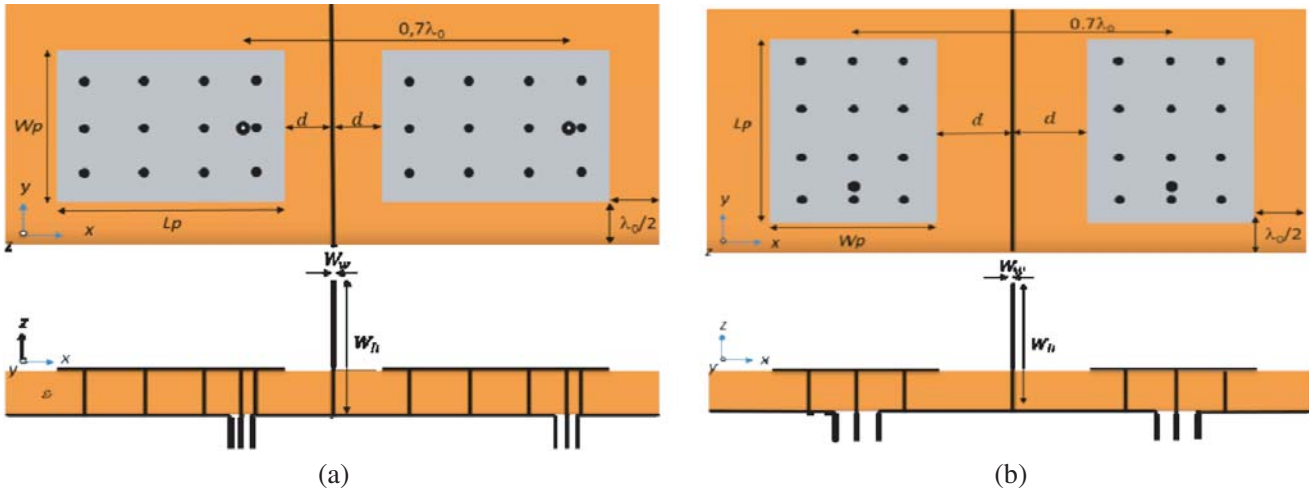


(a) (b)

**Figure 15.** Top and side view of pin loaded two patch antennas with metallic wall barrier oriented along: (a) $E$-plane; (b) $H$-plane.

Figure 16(a) and Figure 16(b) show the corresponding $S$-parameters in $E$- and $H$-planes, respectively. It can be observed that the rejection band presents wide-band characteristics with $-44.89$ dB and $-42.14$ dB of coupled power in $E$- and $H$-planes, respectively, at the resonant frequency. Here, combination of pin loaded patch antennas with metallic wall presents almost 23 dB and 15 dB less coupled power than conventional patch antenna array arranged along $E$- and $H$-planes, respectively.

### 3.5. Realization of Pin Loaded Patch Antenna Array with Metallic Wall Oriented along *E*- and *H*-Planes

The pin loaded patch antenna array with metallic walls barriers arranged along $E$- and $H$-planes has been manufactured to validate 3D simulation results (Figure 17). The pin loaded antennas with metallic walls oriented along $E$- and $H$-planes show a mutual coupling ($S_{12–21}$) approximately $-39.18$ dB and $-44.05$ dB, respectively, with wide-band rejection characteristics (Figures 18(a)–(b)). It can be observed

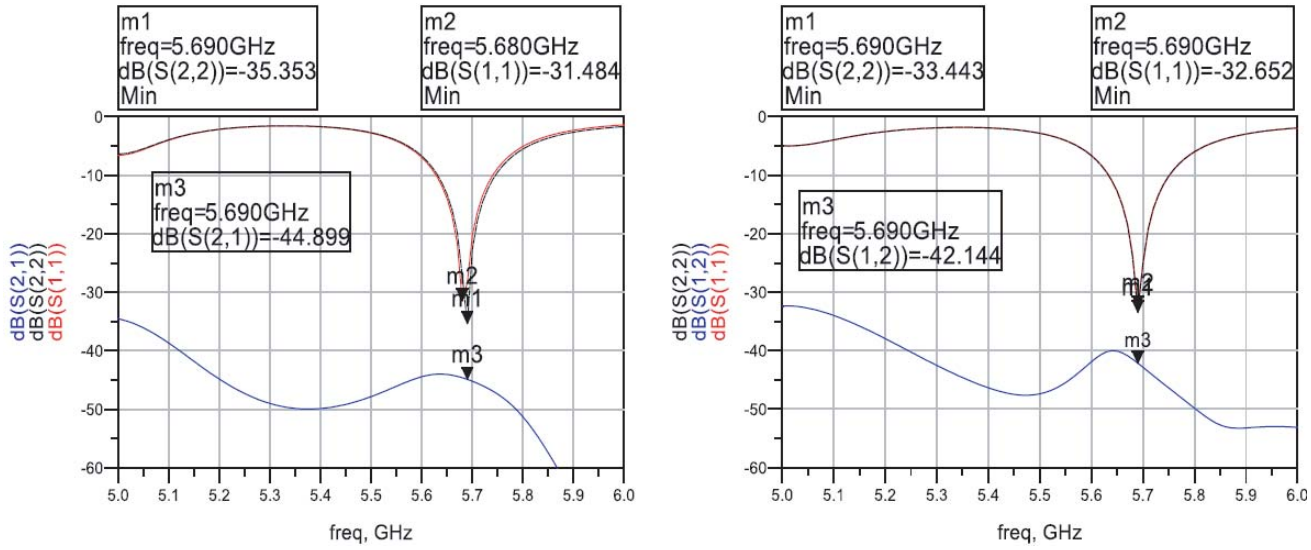


**Figure 16.** Simulated $S$-parameters of pin loaded two antennas with metallic wall barrier oriented along: (a) $E$-plane; (b) $H$-plane.

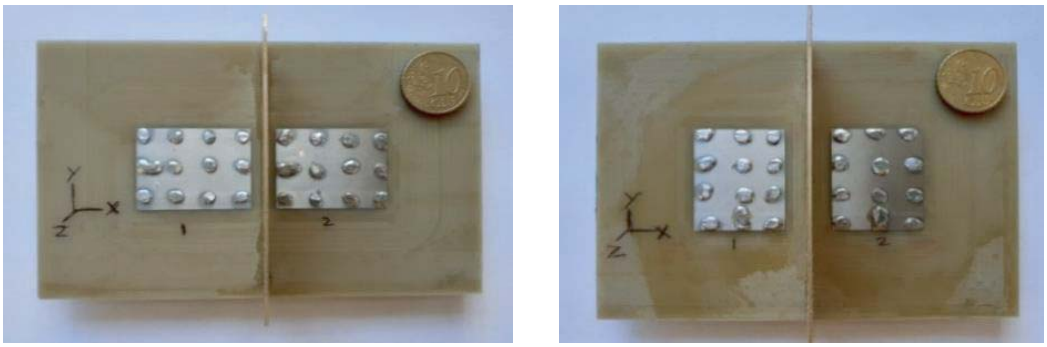


**Figure 17.** Fabricated Pin loaded two element antenna arrays with metallic wall barrier oriented along: (a) $E$-plane; (b) $H$-plane.

that the antennas in both planes resonate slightly at lower frequencies (5.56 GHz) than the reference pin loaded antenna (5.69 GHz) due to manufacturing tolerance. Anyway, slight variation in resonant frequencies does not affect the observance of our results.

The measured radiation patterns of the array with a metallic wall oriented along $E$- and $H$-planes are shown in Figure 19(a) and Figure 19(b), respectively. The array in both orientations shows efficient radiation characteristics despite insertion of metallic walls.

It can be observed that the realized array presents almost 5 dB more coupled power in $E$-plane than the coupled power through 3D simulation. The $H$-plane realized array presents almost 2 dB less coupled power than 3D simulation. This little variation of coupled power in simulation and realization is the result of manufacturing tolerance and measurement setup in realized arrays. It can also be observed through Figure 18 that the rejection band ($S_{12}$) in both orientations is quite wide and remains almost less than $-40$ dB in the entire frequency band.

Table 2 provides the comparative analysis of mutual coupling through 3D simulation and realization among conventional patch antenna arrays, pin loaded patch antenna arrays, and the combination of pins and metallic wall barrier patch antenna arrays in both planes of orientations.

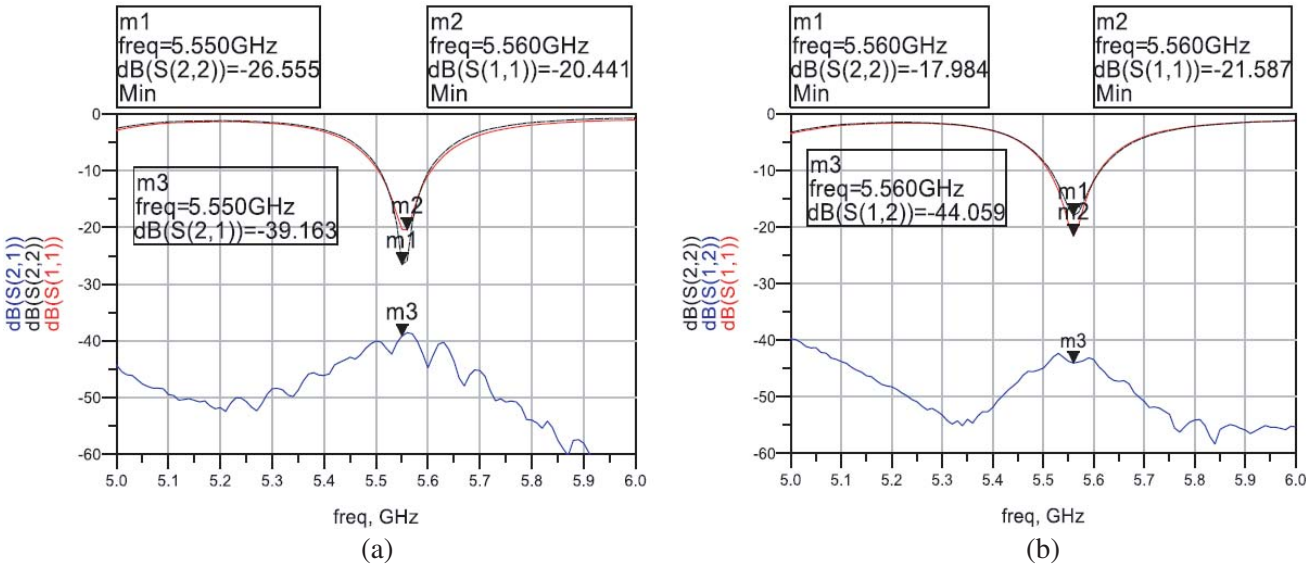


**Figure 18.** Measured $S$-parameters of pin loaded two antennas with metallic wall barrier oriented along: (a) $E$-plane; (b) $H$-plane.

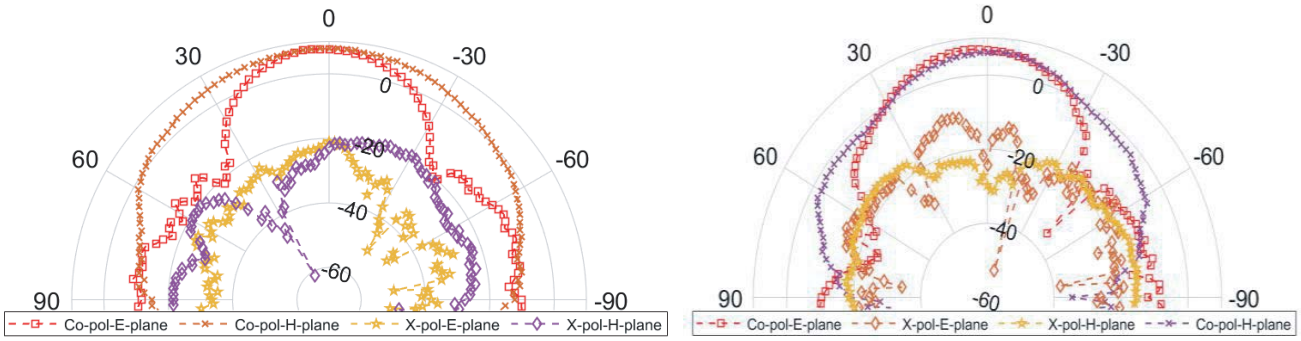


**Figure 19.** Measured radiation pattern of pin loaded patch antenna array with walls oriented along: (a) $E$-plane; (b) $H$-plane.

**Table 2.** Summarized comparative analysis on the reduction of mutual coupling among conventional patch antennas, pin loaded patch antennas and pin loaded patch antennas with metallic wall barrier in $E$- and $H$-plane orientations.

| Two Element patch antenna array | $S_{12\,(\mathrm{dB})}$ via 3D Simulation | $S_{12\,(\mathrm{dB})}$ via Realization |
|---|---|---|
| Conventional patches$_{(E\text{-plane})}$ | $-21.03$ | $-21.56$ |
| Conventional patches$_{(H\text{-plane})}$ | $-27.45$ | $-29.50$ |
| Pin loaded patches$_{(E\text{-plane})}$ | $-26.04$ | - |
| Pin loaded patches$_{(H\text{-plane})}$ | $-31.64$ | - |
| Pin loaded patches with wall$_{(E\text{-plane})}$ | $-44.89$ | $-39.18$ |
| Pin loaded patches with wall$_{(H\text{-plane})}$ | $-42.14$ | $-44.06$ |

It can be observed that the proposed designs in $E$-plane and $H$-plane improve isolation by 19 dB and 15 dB, respectively, through measurement, as compared to conventional patch antenna arrays.

### 3.6. Parametric Analysis of the Effect of Mutual Coupling with Respect to Height of the Metallic Wall

A parametric analysis of the variation in level of mutual coupling with respect to height of the wall has been carried out in both $E$- and $H$-planes as shown in Figure 20. It has been observed that a variation in height of the wall ($W_h$) produces a linear shift in transmission coefficient for this particular design. As the height of the wall is increased, a tendency of low mutual coupling is observed in $H$-plane, while in $E$-plane the tendency of coupling reduction continues till 35 mm ($\sim 0.7\lambda_0$). It appears that the effect of the height of metallic wall in $E$-plane shows no better reduction if the height is raised more than $0.7\lambda_0$.

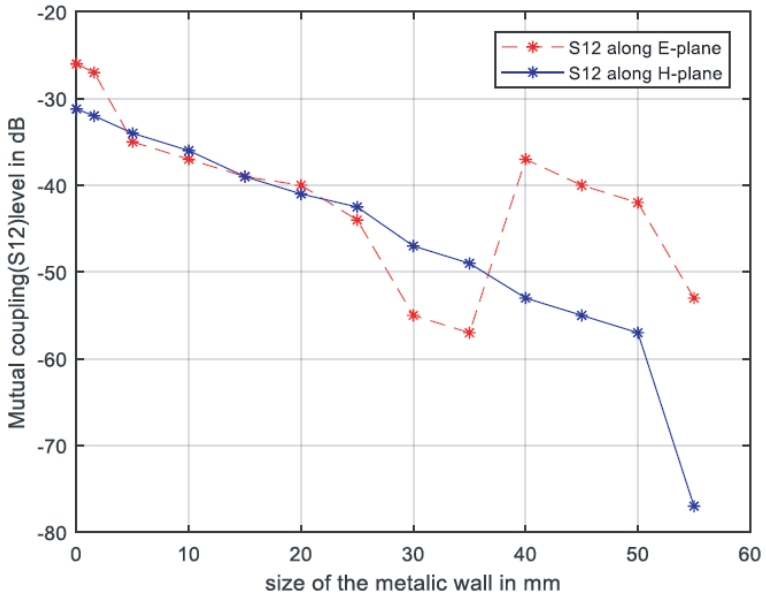


**Figure 20.** Parametric analysis of mutual coupling variation with respect to the wall height ($W_h$) in pin loaded patch antenna arrays oriented along $E$-plane and $H$-plane.

### 3.7. Surface Current Distribution and E-Field Analysis

Figures 21(a)–(d) show the surface current distribution in conventional and pin loaded patch antenna array in both $E$- and $H$-plane orientations. In this case, one antenna is powered on while the other is matched loaded. It can be observed that the conventional antenna array shows surface current

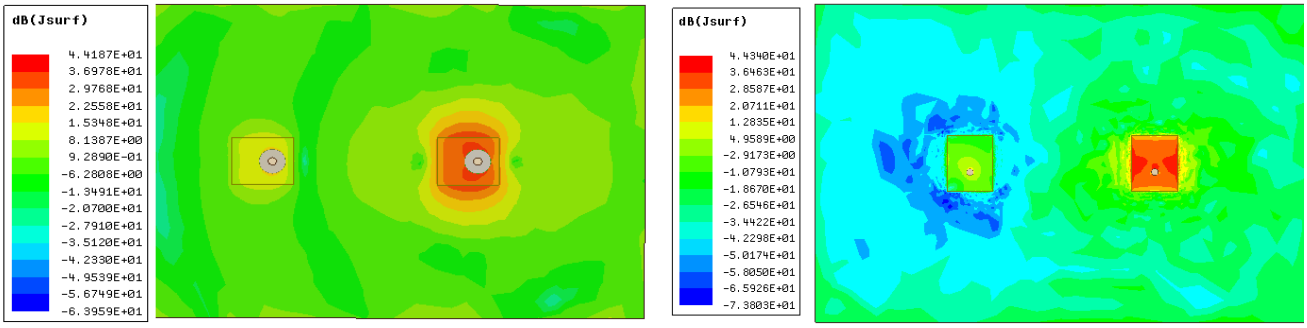


(a) (b)

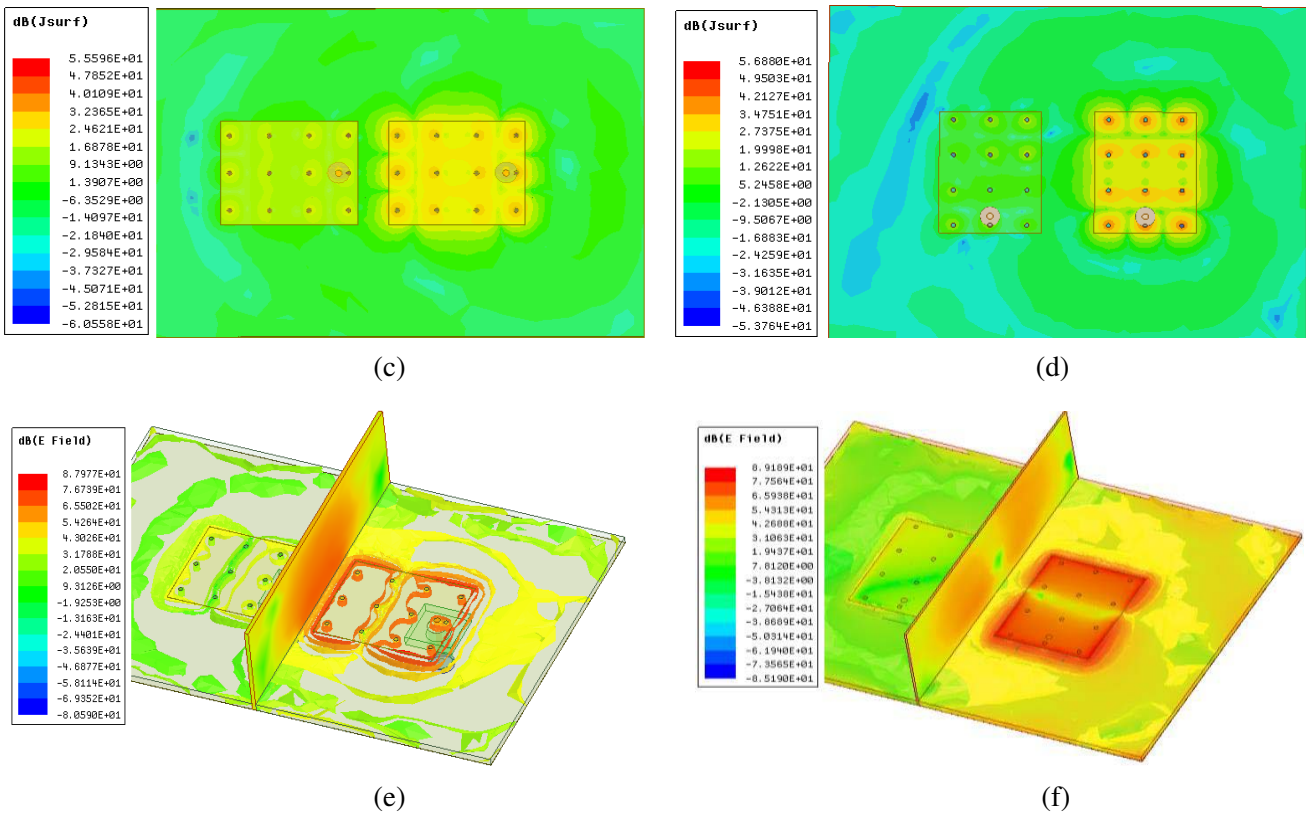


**Figure 21.** (A) Surface current distribution in: (a) Conventional patch antenna array oriented along $E$-plane; (b) Conventional patch antenna array oriented along $H$-plane; (c) Pin loaded patch antenna array oriented along $E$-plane; (d) Pin loaded patch antenna array oriented along $H$-plane; (B) $E$-field intensity in Pin loaded patch antenna array with metallic wall oriented along: (e) $E$-plane; (f) $H$-plane.

penetration from one antenna to another while pin loaded patch antenna array presents negligible amount of surface current penetration. Figures 21(e)–(f) show that the $E$-field is well shielded by the introduction of metallic walls.

## 4. CONCLUSIONS

In this paper, a pin loaded patch antenna has been shown to outperform a conventional patch antenna in terms of suppressing surface waves and radiation in horizontal directions resulting in better directivity. Moreover, when these pin loaded patch antennas are set in arrays, they share 5 dB and 4 dB less coupled power than the conventional patch antenna array arranged along $E$- and $H$-plane orientations, respectively. For further reduction of coupling, pin loaded patch antenna arrays are complemented with metallic walls erected in between the antenna elements to reduce the effect of free space waves coupling. When a combination of pins and metallic wall is utilised, reductions of 19 dB and 15 dB in $E$-plane and $H$-plane, respectively, have been observed through measurement at the resonant frequency. It has also been shown that apart from the suppression of mutual coupling, this technique presents a wide-band rejection characteristic of transmission coefficient along both $E$- and $H$-plane orientations with efficient radiation characteristics. The studied two-element directive array can be extended to any larger linear or planar array configurations.

## ACKNOWLEDGMENT

Authors would like to thank Engr. Marc Brunet for manufacturing antenna prototypes.

## REFERENCES


1. Islam, M. T. and M. S. Alam, "Compact EBG structure for alleviating mutual coupling between patch antenna array elements," *Progress In Electromagnetic Research*, Vol. 137, 425–438, 2013.
2. Monavar, F. M. and N. Komjani, "Bandwidth enhancement of microstrip patch antenna using jerusalem cross-shaped frequency selective surfaces by invasive weed optimization approach," *Progress In Electromagnetic Research*, Vol. 121, 103–120, 2011.
3. Lalbakhsh, A., M. U. Afzal, K. P. Esselle, and S. L. Smith, "A high-gain wideband EBG resonator antenna for 60 GHz unlicenced frequency band," *12th European Conference on Antennas and Propagation (EuCAP 2018)*, 10–12, 2018.
4. Lalbakhsh, A., M. U. Afzal, K. P. Esselle, S. L. Smith, and B. A. Zeb, "Single-dielectric wideband partially reflecting surface with variable high-gain resonant cavity antenna," *IEEE Trans. Antennas Propag.*, Vol. 67, No. 3, 1916–1921, 2019.
5. Lalbakhsh, A., M. U. Afzal, K. P. Esselle, and S. L. S. Member, "Low-cost nonuniform metallic lattice for rectifying aperture near-field of electromagnetic bandgap resonator antennas," *IEEE Trans. Antennas Propag.*, Vol. 68, No. 5, 3328–3335, 2020.
6. Dubost, G., "Influence of surface wave upon efficiency and mutual coupling between rectangular microstrip antennas," *International Symposium on Antennas and Propagation Society, Merging Technologies for the 90's, Dallas, TX, USA*, 660–663, 1990.
7. Pozar, D. M. and P. R. Haddad, "Anomalous mutual coupling between microstrip antennas," *IEEE Trans. Antennas Propag.*, Vol. 42, No. 11, 1545–1549, 1994.
8. Djordjevic, A. R. and M. M. Nikolic, "Microstrip antennas with suppressed radiation in horizontal directions and reduced coupling," *IEEE Trans. Antennas Propag.*, Vol. 53, No. 11, 3469–3476, 2005.
9. Hou, D., S. X. B. Wang, L. J. J. Wang, and W. Hong, "Elimination of scan blindness with compact defected ground structures in microstrip phased array," *IET Microwaves, Antennas Propag.*, Vol. 3, No. 2, 269–275, 2009.
10. Tang, S. X. M. and Y. B. S. Gao, "Mutual coupling suppression in microstrip array using defected ground structure," *IET Microwaves, Antennas Propag.*, Vol. 5, No. 12, 1488–1494, 2011.
11. Yang, F. and Y. Rahmat-samii, "Microstrip antennas integrated with Electromagnetic Band-Gap (EBG) Structures: A low mutual coupling design for array applications," *IEEE Trans. Antennas Propag.*, Vol. 51, No. 10, 2936–2946, 2003.
12. Rajo-iglesias, E., S. Member, Ó. Quevedo-teruel, S. Member, and L. Inclán-sánchez, "Mutual coupling reduction in patch antenna arrays by using a planar EBG structure and a multilayer dielectric substrate," *IEEE Trans. Antennas Propag.*, Vol. 56, No. 6, 1648–1655, 2008.
13. Beiranvand, E., M. Afsahy, and V. Sharbati, "Reduction of the mutual coupling in patch antenna arrays based on EBG by using a planar frequency-selective surface structure," *Int. J. Microw. Wirel. Technol.*, Vol. 9, No. 2, 349–355, 2015.
14. Qiu, L., F. Zhao, K. Xiao, S. Chai, and J. Mao, "Transmit-Receive isolation improvement of antenna arrays by using EBG structures," *IEEE Antennas Wirel. Propag. Lett.*, Vol. 11, 93–96, 2012.
15. Sahandabadi, S. and S. V. A.-D. Makki, "Mutual coupling reduction using complementary of SRR with wire MNG structure," *Microw. Opt. Technol. Lett.*, Vol. 61, No. 5, 1231–1234, 2019.
16. Mohamadzade, B., A. Lalbakhsh, R. B. V. B. Simorangkir, A. Rezaee, and R. M. Hashmi, "Mutual coupling reduction in microstrip array antenna by employing cut side patches and EBG structures," *Progress In Electromagnetic Research*, Vol. 89, 179–187, 2020.
17. Farsi, S., et al., "Mutual coupling reduction between planar antennas by using a simple microstrip U-section," *IEEE Antennas Wirel. Propag. Lett.*, Vol. 11, 1501–1503, 2012.
18. Ali, A., L. Neyestanak, F. Jolani, and M. Dadgarpour, "Mutual coupling reduction between two microstrip patch antennas," *2008 Canadian Conference on Electrical and Computer Engineering, Niagara Falls*, 739–742, 2008.

19. Qi, H., L. Liu, X. Yin, H. Zhao, and W. J. Kulesza, "Mutual coupling suppression between two closely spaced microstrip antennas with an asymmetrical coplanar strip wall," *IEEE Antennas Wirel. Propag. Lett.*, Vol. 15, 191–194, 2016.
20. Arand, B. A., A. Bazrkar, and A. Zahedi, "Design of a phased array in triangular grid with an efficient matching network and reduced mutual coupling for wide-angle scanning," *IEEE Trans. Antennas Propag.*, Vol. 65, No. 6, 2983–2991, 2017.
21. Kiani, M. and H. R. Hassani, "Wide scan phased array patch antenna with mutual coupling reduction," *IET Microwaves, Antennas Propag.*, Vol. 12, No. 12, 1932–1938, 2018.
22. Tang, J., et al., "A metasurface superstrate for mutual coupling reduction of large antenna arrays," *IEEE Access*, Vol. 8, 126859–126867, 2020.
23. Zhang, X., S. Member, and L. Zhu, "Gain-enhanced patch antennas with loading of shorting pins," *IEEE Trans. Antennas Propag.*, Vol. 64, No. 8, 3310–3318, 2016.
24. Samanta, S., P. S. Reddy, and K. Mandal, "Cross-polarization suppression in probe-fed circular patch antenna using two circular clusters of shorting pins," *IEEE Trans. Antennas Propag.*, Vol. 66, No. 6, 3177–3182, 2018.
25. Sanad, H., "Effect of the shorting posts on short circuit microstrip antennas," *Proceedings of IEEE Antennas and Propagation Society International Symposium and URSI National Radio Science*, No. 2, 794–797, 1994.
26. Targonski, S. D. and R. B. Waterhouse, "Performance of microstrip patches incorporating a single shorting post," *IEEE Antennas Propag. Soc. Int. Symp.*, No. 1, 29–32, 1996.
27. Kishk, A. A., L. Shafai, and A. Ittipiboon, "Single-element rectangular microstrip antenna for dual frequency operation," *Electron. Lett.*, Vol. 19, No. 8, 298–300, 1983.
28. Shuley, N. V. and R. B. Waterhouse, "Dual frequency microstrip rectangular patches," *Electron. Lett.*, Vol. 28, No. 7, 606–607, 1992.
29. Guha, D., S. Member, and Y. M. M. Antar, "Circular microstrip patch loaded with balanced shorting pins for improved bandwidth," *IEEE Antennas Wirel. Propag. Lett.*, Vol. 5, 217–219, 2006.
30. Abdullah, M., Q. Li, W. Xue, G. Peng, and Y. He, "Isolation enhancement of MIMO antennas using shorting pins," *Journal of Electromagnetic Waves and Applications*, Vol. 33, No. 10, 1–15, 2019.
31. Li, W., P. Li, and J. Zhou, "Control of higher order harmonics and spurious modes for microstrip patch antennas," *IEEE Access*, Vol. 6, 34158–34165, 2018.